LIDAR AND AERONET MEASUREMENTS IN RIO GALLEGOS, PATAGONIA ARGENTINA

L. Otero[1,6], P. Ristori[2], J. Salvador[1,3], R. D'Elia[1], J. Pallota[1,4] , E.Wolfram[1], B. Holben[5], E. Quel[1]

1. CEILAP (CITEFA-CONICET) - Juan B. de La Salle 4397 - B1603ALO Villa Martelli, Argentina. E-mail: quel@citefa.gov.ar
2. Laboratoire de Pollution de l'Air et du Sol, École Polytechnique Fédérale de Lausanne, Suisse. E-mail: pablo.ristori@epfl.ch
3. Fellow of Universidad Nacional de San Martin, Buenos Aires, Argentina. E-mail: jsalvador@citefa.gov.ar
4. Fellow of Auger Observatory, Malargüe, Argentina AUGER. E-mail: jpallota@citefa.gov.ar
5. NASA Goddard Space Flight Center, Greenbelt, Maryland, U.S.A. E-mail: brent@aeronet.gsfc.nasa.gov
6. CONAE - Av Paseo Colón 751 - C1063ACH Buenos Aires, Argentina. E-mail: lotero@citefa.gov.ar

ABSTRACT
As part of the SOLAR field campaign, the CEILAP (CITEFA – CONICET), has developed a mobile tropospheric aerosol lidar system placed in a shelter. This campaign took place in the southern winter-spring period 2005, at Río Gallegos (51,9° S, 69,1° W, 15 m ASL), in Patagonia, Argentina. This lidar and a sunphotometer provided by AERONET (NASA), were used to study aerosols optical properties and boundary layer temporal evolution. This intensive field campaign was supported by JICA, Japan International Cooperation Agency [1], to obtain simultaneous measurements of ozone, water vapor, aerosols vertical profiles and related parameters.

1. INTRODUCTION

The atmospheric composition plays an essential role in human life with global and regional changes because the atmosphere links all of the principal components of the Earth system. Aerosols are particles in suspension in the air which can be located in a mixture with atmospheric components in liquid and gaseous phases. The origins of these are anthropogenic, biomass burning, dust, volcanic, sea salt, etc. Aerosol optical properties studies are important for their direct an indirect radiative effect in the global climate system [2].

2. INSTRUMENTS

The mobile tropospheric lidar system was conceived to monitor range-resolved aerosol optical properties from the IR to the near UV spectral region. Its measuring range, from 300 m to 10 km ASL, allows studying the complete tropospheric aerosol column. The LIDAR emission system is a 30 Hz – 130 mJ (355 nm) solid state Nd:YAG laser (QUANTEL 980) with 0.6 mrad beam divergence. The backscattered radiation is collected by an f/2, 1 m focal length newtonian telescope and focused into a 1 mm diameter optical fiber. The laser is sent parallel to reception system optical axis at a distance of about 30 cm; therefore the blind zone is approximately 300 m. The system scheme is described in [1]. Other lidars configurations are used in the SOLAR campaign to measure stratospheric ozone and tropospheric water vapor.

AERONET (NASA) is a federated international network of sun/sky radiometers [3, 4]. Data are available online in near real-time mode [5], and the measurements reported in this paper were made with the automatic scanning sunphotometer CIMEL described in [3], installed at Río Gallegos site on November 2005. The data are available with a confidence level of 1.5 (automatic operation with a cloud-screened procedure) [5, 6].
At the same site are installed also UVA and UVB radiometers, a GUV narrow band radiometer, a pyranometer and a meteorological station [1].

3. RESULTS

With the instruments mentioned above, three interesting cases of aerosols load were analyzed in this work, produced during the spring period in 2005.

3.1. Event I: September 29, 2005.

Figs. 1 and 2 show the normalized aerosol backscatter at 1064 nm during the morning and the evening of September 29, 2005. We can observe the nocturnal boundary layer, the entrainment zone and the evolution of the diurnal boundary layer starting at 11 h. Fig. 3 compares the normalized backscatter profile at 1064 nm with the potential temperature. The sounding was obtained from the nearest sounding place at Mount Pleasant Airport, Malvinas Islands (51.5 S, 58.3 W, 74 m ASL). Both measurements were taken at the same time (9 h local time), and the signals presents the same signature. Meteorological data is shown in Figs. 4, 5 and 6. We can observe the wind speed temporal evolution in Fig. 4. The wind speed minimum is 1.6 km/h and maximum is 32.2 km/h. The wind direction illustrated in Fig. 5 shows a W preferential direction in the morning and a NNE in the evening. In Fig. 6 we can see how the atmospheric pressure rises during the morning.

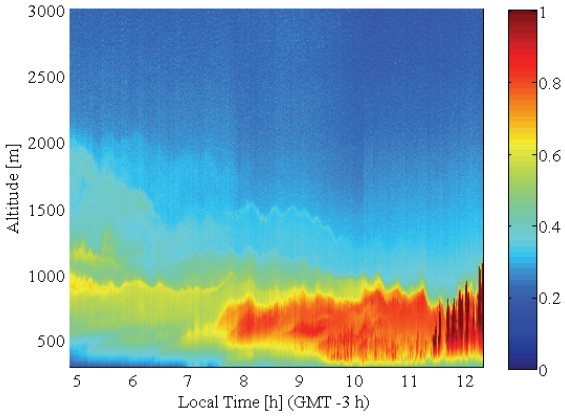

Fig. 1. Normalized aerosol backscatter at 1064 nm during the morning (September 29, 2005).

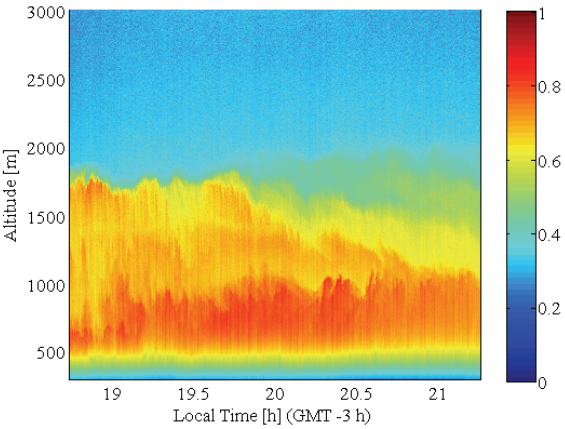

Fig. 2. Normalized aerosol backscatter at 1064 nm during the evening (September 29, 2005).

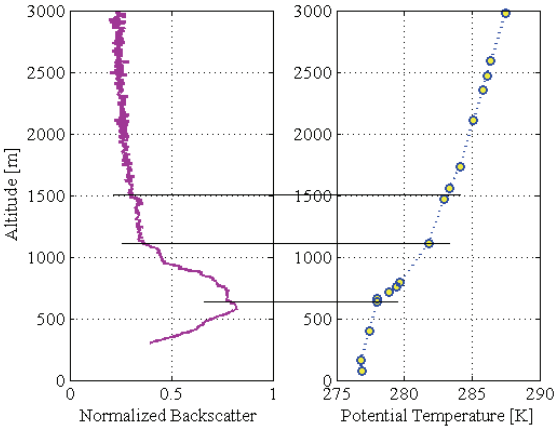

Fig. 3. Normalized backscatter at 1064 nm and potential temperature, both measured at the same time (9 h local time, September 29, 2005).

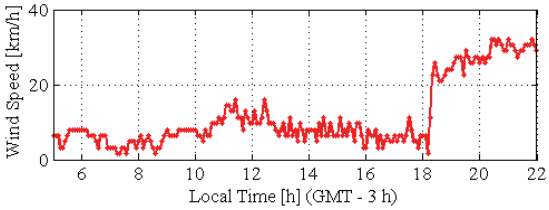

Fig. 4. Wind speed evolution (September 29, 2005).

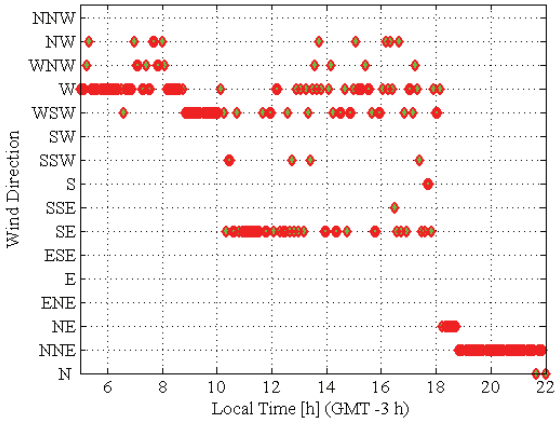

Fig. 5. Wind direction evolution (September 29, 2005).

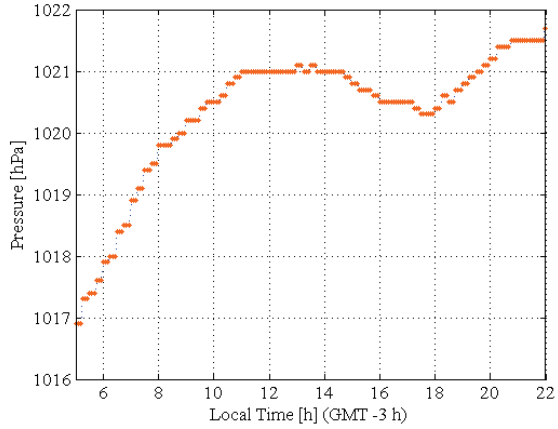

Fig. 6. Atmospheric pressure evolution(September 29, 2005).

3.2. Event II: October 26, 2005.

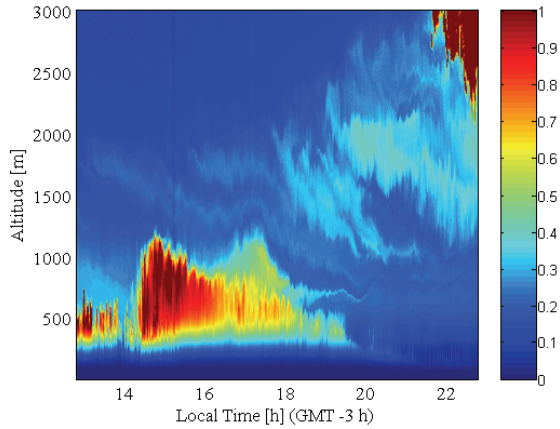

Fig. 7. Normalized aerosol backscatter at 1064 nm (October 26, 2005).

Fig. 7 shows a normalized aerosol backscatter profile measured at 1064 nm. The evolution of the boundary layer in height during the morning and its subsidence during the afternoon can be seen. The arrival of many aerosol layers are detected between 1000 and 2500 m. At 22 h local time a cloud is observed at 3000 m. Fig. 8 shows a slight decrease on the atmospheric pressure. An

important change in the wind direction (from SW to SE) is observed in Fig. 9. We can see the wind speed temporal evolution in Fig. 10. The wind speed minimum is 8 km/h and maximum is 29 km/h.

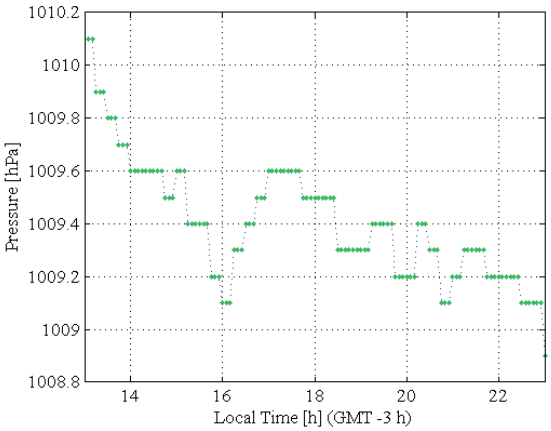

Fig. 8. Atmospheric pressure (October 26, 2005).

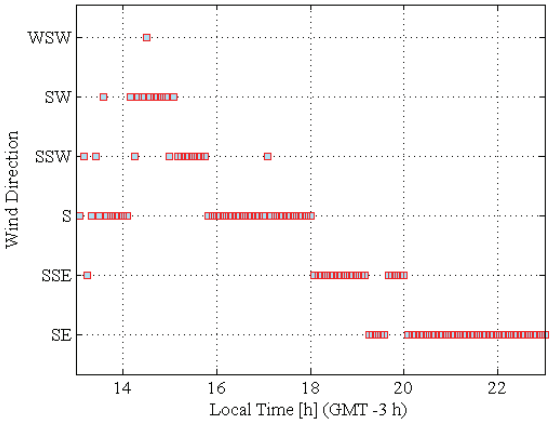

Fig. 9. Wind direction evolution (October 26, 2005).

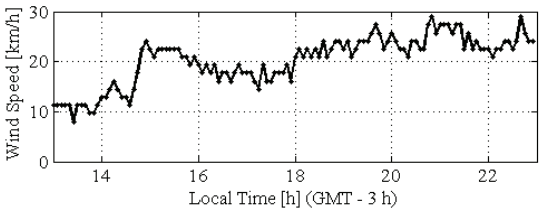

Fig. 10. Wind speed evolution (October 26, 2005).

3.3. Event III: November 14, 2005.

Fig. 11 shows the normalized aerosol backscatter at 1064 nm for November 14, 2005. We can observe a strange behaviour of the boundary layer and the arrival of aerosol layers between 1500 and 3000 m. In Fig 12 the AOT evolution at 440 nm is shown. Fig. 13 presents a plot of the AOT (440 nm) vs. Ångström coefficient, with a distribution corresponding to Antarctic aerosols [7, 8]. Fig. 14 shows the Ångström coefficient and water vapor content evolution during the day. The important anticorrelation of these measurements suggests the arrival of big aerosols of hydroscopic nature.

In Fig. 15 we can see how the atmospheric pressure disminished approximately 1 hPa between 13 to 16 h local time. The wind direction changed at 14:30 h local time from S to SE. (Fig. 16). We can observe the wind speed temporal evolution in Fig. 17. The wind speed minimum is 6.4 km/h and maximum is 27.4 km/h.

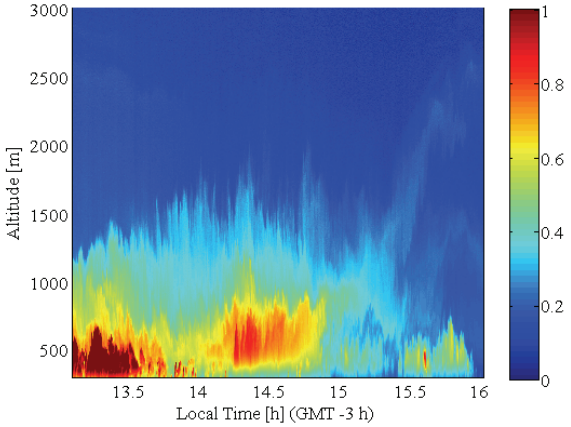

Fig. 11. Normalized aerosol backscatter at 1064 nm (November 14, 2005).

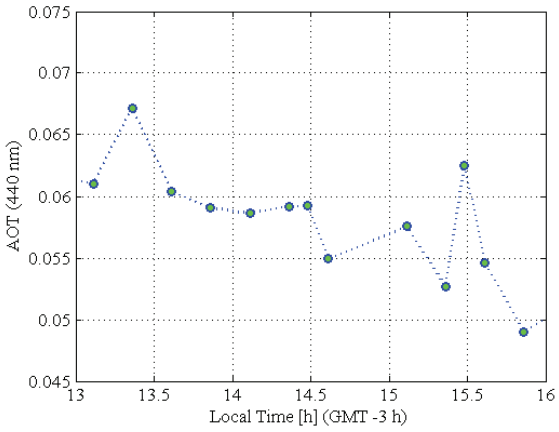

Fig. 12.Temporal evolution of AOT at 440 nm (November 14, 2005).

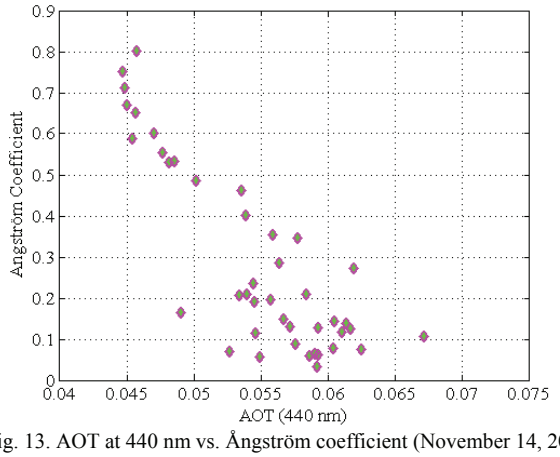

Fig. 13. AOT at 440 nm vs. Ångström coefficient (November 14, 2005).

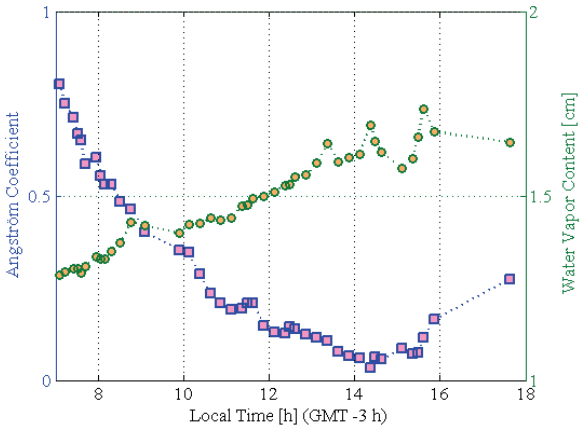

Fig. 14. Ångström coefficient and water vapor content temporal evolution (November 14, 2005).

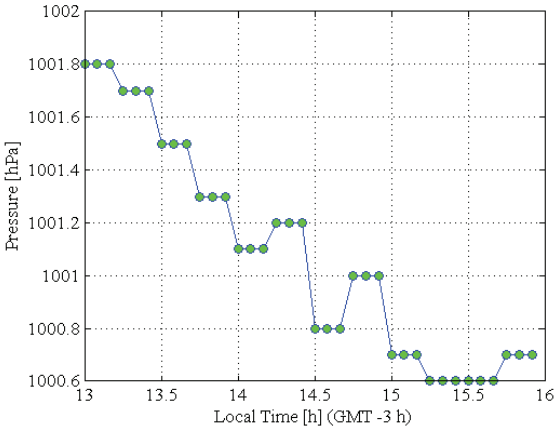

Fig. 15. Atmospheric pressure evolution (November 14, 2005)

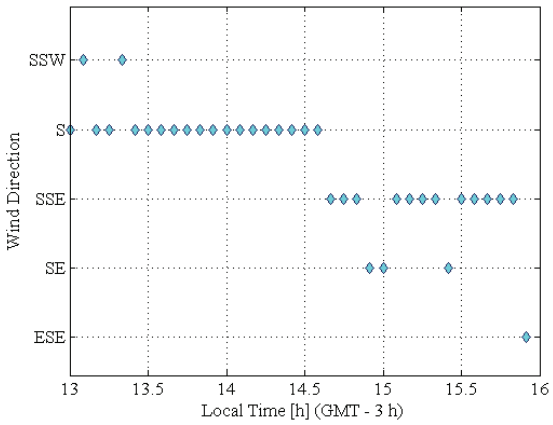

Fig. 16. Wind direction evolution. (November 14, 2005).

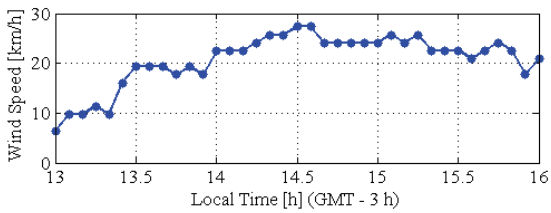

Fig. 17. Wind speed evolution. (November 14, 2005).

4. CONCLUSIONS

We present the first ground based lidar and aerosols total column measurements in Patagonia. We can observe in the first case study an important boundary layer evolution almost reaching 2000 m AGL with a significant subsidence in the evening. Next two cases show the wind affecting the boundary layer evolution. In all cases the wind direction plays a major role in our study since it introduces different kind of particles to the boundary layer and upper layers. The aerosol properties study reveals the major presence of Antarctic aerosols is with AOT (440 nm) < 0.1 and Ångström coefficient < 0.8.

5. ACKNOWLEDGMENTS

Authors thanks to the following institutions: JICA, for the economical support of the SOLAR Field Campaign, NASA for (AERONET network), CONICET, ANPCyT, CONAE and especially to Dr. Marcos Machado for the provided support in the realization of this work.

6. REFERENCES

1. http://www.division-lidar.com.ar/

2. Andreae M. O. *Climatic effects of changing atmospheric aerosol levels en World Survey of Climatology* vol 16, Future Climates of the World, A. Henderson-Sellers, 341-392 Elsevier, New York, 1995.

3. Holben B., T. F. Eck, I. Slutsker, D. Tanre, J. P. Buis, A. Setzer, E. Vermote, J. A. Reagan, Y. Kaufman, T. Nakajima, F. Lavenu, I. Jankowiak, and A. Smirnov. AERONET- A federated instrument network and data achieve for aerosol characterization, *Remote Sens*. 12, 1147-1163, 1998.

4. Holben B. N., D. Tanre, A. Smirnov, T. F. Eck, I. Slutsker, N. Abuhassan, W. W. Newcomb, J. Schafer, B. Chatenet, F .Lavenue, Y. J. Kaufman, J. Vande Castle, A. Setzer, B. Markham, D. Clark, R. Frouin, R. Halthore, A. Karnieli, N. T. O'Neill, C .Pietras, R. T. Pinker, K. Voss, and G. Zibordiet. An emerging ground based aerosol climatology: Aerosol optical depth from AERONET, *J. Geophys. Res*., 106, 2,067– 12,097, 2001.

5. http:// aeronet.gsfc.nasa.gov/

6. Dubovik O. and M. King. A flexible inversion algorithm for retrieval of aerosol optical properties from Sun and sky radiance measurements. *J. Geophys. Res.*, Vol. 105, No. D16, Pages 20,673-20,696, 2000.

7. Hess M., P. Koepke, I. Schult. Optical Properties of Aerosols and Clouds: The Software Package OPAC. *Bulletin of the American Meteorological Society* 831 - 844 Vol. 79, No. 5, 1998.

8. Otero, L., P. Ristori, B. Hoben, E. Quel. Espesor óptico de aerosoles durante el año 2002 para distintas estaciones pertenecientes a la red AERONET – NASA Anales AFA 2005. (In Press)